Developing a framework towards global biochar supply chains to optimize regional production cost

Kern, Johannes; Abdelshafy, Ali; Walther, Grit

DOI
10.1016/j.eti.2025.104658

Publication date
2025

Document Version
Final published version

Published in
Environmental Technology and Innovation

Citation (APA)
Kern, J., Abdelshafy, A., & Walther, G. (2025). Developing a framework towards global biochar supply chains to optimize regional production cost. *Environmental Technology and Innovation*, *40*, Article 104658. https://doi.org/10.1016/j.eti.2025.104658

Environmental Technology & Innovation 40 (2025) 104658

Contents lists available at ScienceDirect

Environmental Technology & Innovation

journal homepage: www.elsevier.com/locate/eti

Developing a framework towards global biochar supply chains to optimize regional production cost

Johannes Kern [a,*], Ali Abdelshafy [b], Grit Walther [a]

[a] RWTH Aachen University, Chair of Operations Management, Kackertstraße 7, Aachen 52072, Germany
[b] Delft University of Technology, Energy and Industry Group, Faculty of Technology Policy and Management, Jaffalaan 5, Delft 2628 BX, the Netherlands

ARTICLE INFO

Keywords:
Biochar
Carbon dioxide removal
Lignocellulosic biomass
Techno-economic analysis
Spatial modeling
Pyrolysis technologies

ABSTRACT

The expansion of carbon dioxide removal (CDR) strategies is essential to achieve the climate targets. Among emerging CDR technologies, biochar holds particular promise due to its stable carbon storage and multiple co-benefits. While previous studies have examined the global potentials of biochar production, comprehensive assessments that include cost structures and spatial variability remain limited. This study addresses this gap and presents a comprehensive that integrates geospatial machine learning with techno-economic analysis to estimate region-specific biochar production costs at a global level. The derived approach estimates the biomass yields of various lignocellulosic biomass sources using an XGBoost machine learning model trained on climate and soil data. Roadside production costs are then calculated based on resource input parameters, followed by transport cost estimations using spatial distance metrics. Finally, pyrolysis costs are included to derive the total production cost of biochar per ton across regions globally. The results show substantial regional variation, with total production costs ranging from 113 to over 1500 €/ton. Sub-Saharan Africa, Latin America, and South Asia demonstrate the lowest median costs, below 300 €/ton, primarily due to low labor and biomass costs. Eucalyptus emerges as the most cost-efficient biomass provided it is cultivated. While the Kontiki flame curtain kilns are more cost efficient in low-income regions, advanced-technology plants become competitive in industrialized areas, especially when district heat is considered. These insights are crucial for guiding investments and policies that aim to expand biochar use as a viable and cost-effective CDR pathway.

1. Introduction

Extensive research on global climate prediction shows that anthropogenic carbon emissions are driving global temperature increases, leading to more frequent extreme weather events and other climate impacts (IPCC, 2023). These emissions primarily originate from fossil fuel use, land-use changes, energy production, and industrial activities (Smith et al., 2024). To mitigate these impacts, global climate policy under the Paris Agreement has set the goal of limiting global temperature increases to well below 2°C above pre-industrial levels, ideally even limiting the increase to 1.5°C. Meeting this goal requires both significant carbon emissions reductions and atmospheric carbon removal (Smith et al., 2024), with at least 7 Gt of CO_2 removal capacity needed annually by 2050

* Corresponding author.
E-mail address: johannes.kern@om.rwth-aachen.de (J. Kern).

https://doi.org/10.1016/j.eti.2025.104658
Received 9 September 2025; Received in revised form 5 November 2025; Accepted 25 November 2025
Available online 26 November 2025

(Breunig et al., 2023). Although many countries have derived policies to promote carbon dioxide removal (CDR) supply chains (Ehsan et al., 2024; Kirchem and Schill, 2023; Wolniak and Skotnicka-Zasadzień, 2023), CDR applications remain scarce in the market, requiring comprehensive technical evaluations to inform national and regional decision-making.

According to Smith et al. (2024), five novel CDR technologies have reached medium to high technology readiness level, having been demonstrated in industrially relevant settings. These technologies are biochar, mineral products, bio-oil storage, bioenergy with carbon capture and storage (BECCS), and direct air carbon capture and storage (DACCS). Among them, biochar has drawn significant attention as a stable form of solid carbon produced through high-temperature biomass conversion under low-oxygen conditions (Adhikari et al., 2024). Unlike other CDR applications, biochar offers multiple co-benefits beyond carbon sequestration. For example, biochar can be used as a soil amendment to enhance soil fertility, a reducing agent in metallurgy, an additive in manufactured products, and a replacement for fossil fuels in thermal and electrical energy generation, as well as in other industrial processes (Azzi et al., 2021; Song et al., 2023). As a result, biochar constitutes the largest share of global CDR capacity currently, accounting for approximately 0.008 $GtCO_2$ of the total 0.013 GtCO2 per year (Smith et al., 2024).

Hence, the production potential and carbon removal capacity of biochar has been widely discussed in the literature. For example, several studies have focused on the global availability of residual biomass resources, including agriculture, forestry, manure, and wastewater treatment plants (Karan et al., 2023; Lefebvre et al., 2023; Lehmann et al., 2021; Powis et al., 2023). These studies assumed that if all residual biomass could be converted into biochar, up to 6.3 Gt CO_2 can potentially be sequestered annually. However, their analyses neglected existing biomass value chains or the costs of biochar production. One of the first studies to address biochar production costs on a global scale was conducted by Fuss et al. (2018). In their comparison of various CDR methods, biochar was found to have relatively low production costs, ranging from 30 to 120 USD per ton of CO_2 removed. A subsequent and more granular analysis by Han et al. (2022) examined the production costs across diverse biomass feedstocks such as straw, wood, and manure, as well as varying plant sizes. Their research even demonstrated an additional significant reduction in production costs by adopting larger pyrolysis systems, with costs ranging between 15 and 60 USD per ton of CO_2 removed. However, rising feedstock supply costs have to be anticipated as agricultural waste is increasingly repurposed for multiple climate mitigation strategies (Han et al., 2022). Therefore,

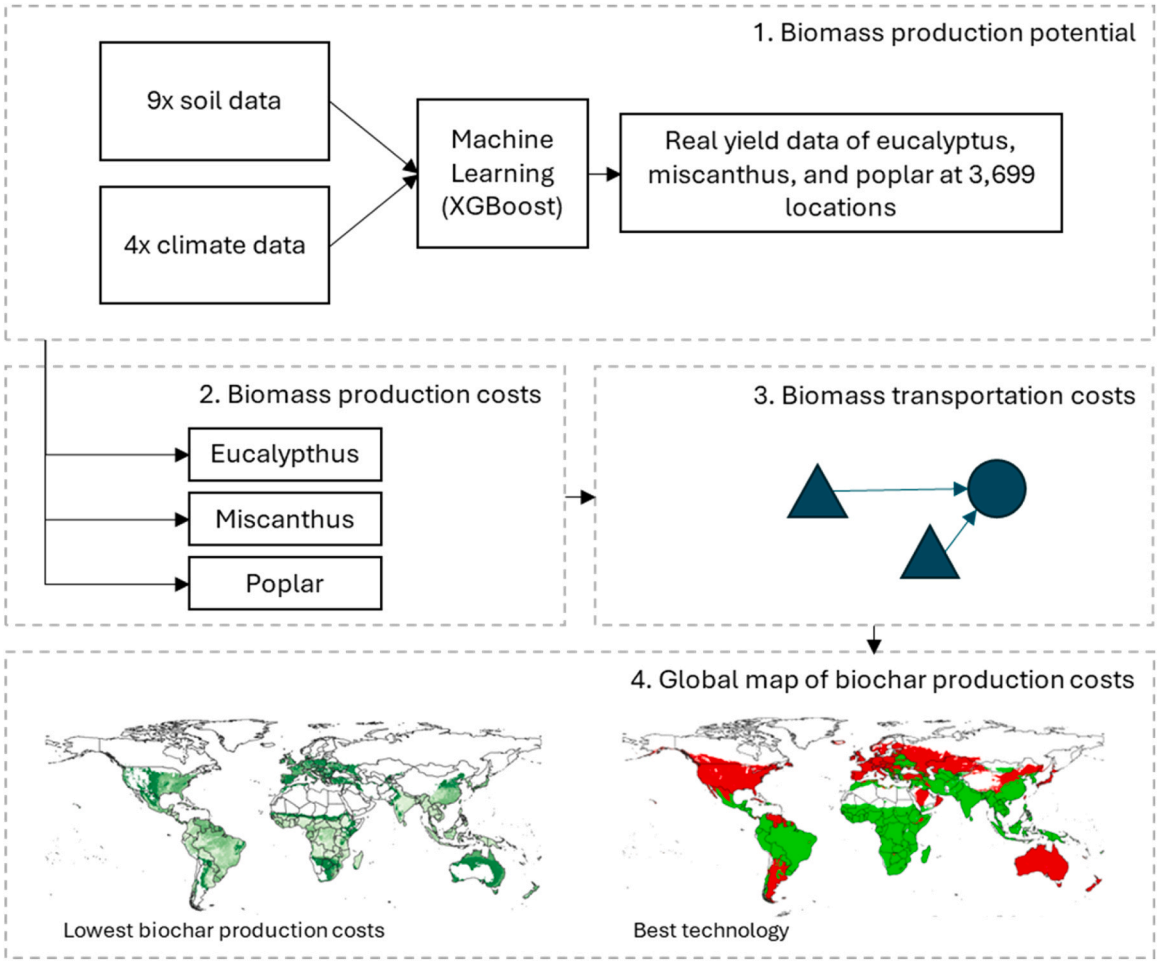

Fig. 1. Methodological framework of our study.

long-term production cost estimates remain uncertain as the valuation of residual biomass is difficult to forecast (Nunes and Silva, 2023).

To avoid conflicts arising from competing utilization pathways of residual biomass, lignocellulosic energy biomass offers a promising alternative for biochar production (Leppäkoski et al., 2021; Mehmooda et al., 2017; Xu et al., 2024). Unlike residual biomass, lignocellulosic biomass bypasses the competition for arable land as it can be grown on globally abundant marginal lands with limited agricultural value due to poor soil quality (Wang et al., 2023). Consequently, increasing research attention has been directed to the production potential and the costs of lignocellulosic biomass through spatial analysis. For example the EU Horizon project S2BIOM developed a spatial database to assess the sustainable costs of supplying lignocellulosic biomass across Europe (Dees et al., 2017). Their findings indicate a production potential of 1090–1420 million tons of biomass per year, with production costs ranging from 40 to 250 €/ton.

To date, studies focusing on production capacity and costs at a global level are limited to upstream phases (i.e. residual biomass), leaving uncertainties regarding downstream stages such as regional biochar production volumes and. Furthermore, existing research lacks clear projections of biochar production volumes at different price points, both at global and national levels. Against this background, this study addresses the identified knowledge gaps by introducing a comprehensive methodology to estimate production costs of biochar. Herein, the derived approach is used to develop a global map highlighting costs of producing biochar from lignocellulosic biomass as feedstock. The study focuses on three dedicated lignocellulosic energy crops (miscanthus, eucalyptus, and poplar) to assess global biochar production potential. Herein, two distinct pyrolysis technologies are also analyzed: a high-tech and low-tech system, allowing for regionalized cost assessments under varying infrastructure conditions. In terms of structure, the subsequent section presents the derived methodological framework and data sources, followed by the results and discussion in Section 3. The final conclusions and policy implications are presented in Section 4.

2. Methodology & materials

To predict the production cost of biochar at a global level, a geospatial model is combined with techno-economic assessment and transportation cost calculation as shown in Fig. 1. First, a geospatial machine learning model is developed to predict the biomass production potential for three lignocellulosic biomass types (miscanthus, eucalyptus, and poplar) based on a global yield dataset developed by (Li et al., 2018) (Section 2.1). Herein, the datasets of the relevant parameters have been collected, and a supervised machine learning algorithm (XGBoost) is used to derive the correlation between the different input parameters and yield. Subsequently, a biomass production cost model is developed based on the studies of (Dees et al., 2017; Panoutsou and Chiaramonti, 2020; Romanelli et al., 2008; Wagner et al., 2022; Winkler et al., 2020) (Section 2.2). As the large-scale pyrolysis technology requires transportation of biomass, average transport distances are determined using the Haversine formula between grid-cell centroids and adjusted by a detour factor of 1.3 to account for realistic road networks (Section 2.3). Finally, the process cost of pyrolysis is included to calculate the total production cost of biochar (Section 2.4). The results are then depicted on a global map to show the biochar production cost under different scenarios (Section 3).

Herein, two different pyrolysis technologies (high-tech and low-tech) are considered to analyze the cost structures under different geographical conditions. The analysis is conducted for a functional unit of 1 ton of biochar. The system boundaries cover the full supply chain from crop cultivation to pyrolysis. This includes cultivation and harvesting on marginal land, roadside handling, biomass transport, and the pyrolysis process, while upstream land-use changes, taxes, and environmental impacts are excluded. All costs are expressed in € [price year 2023]. The four calculation procedures, yield prediction, biomass cost estimation, transport cost modeling, and pyrolysis cost assessment, are summarized in Fig. 1 to illustrate the system scope and workflow.

2.1. Biomass production potential

2.1.1. Data

The global yield dataset used in the study was compiled from 3699 field measurements of three main lignocellulosic bioenergy crops: 846 for eucalyptus, 1421 for miscanthus, and 1432 for poplar (Li et al., 2018). For each yield entry, the dataset contains the location (latitude and longitude), elevation, mean temperature, precipitation, year, and clay content. However, only parts of these yield measurement data provided information on elevation (43 %), mean temperature (36 %), precipitation (51 %), and clay content (14 %) (Li et al., 2018). For the measurements without such information, we filled data gaps with data on the elevation, mean temperature and precipitation data from (Worldclim, 2020) with the mean annual temperature between 1970 and 2000 and the mean annual precipitation between 1970 and 2000, and clay content from (Batjes, 2020).

In addition to mean temperature and precipitation, we also added the Growing Degree Days (GDD) and the Global Aridity Index (GAI), as they are widely used in models predicting agricultural crop yields. They are particularly valuable due to their role in quantifying the plant growing season and water availability (Ma et al., 2023; Schillerberg and Di Tian, 2023). GDD is calculated by subtracting a base temperature (5°C) from the daily mean temperature and dividing the product over a year. Thus, GDD is crucial for accurately predicting agricultural yields, as it plays a key role in identifying the optimal developmental stages of crop plants, which are closely linked to potential yield outcomes (Grigorieva, 2020; Ishikawa et al., 2020). GAI is a vital indicator of aridity, reflecting the balance between temperature and available moisture. This index helps in identifying the favorable environmental conditions for crop cultivation, enabling the prediction of yield outcomes under different climatic scenarios (Ishikawa et al., 2020). Overall, the application of GDD and GAI in addition to mean temperature and precipitation provides a robust framework for modeling and estimating crop productivity in response to climate variables.

In addition to clay content, several other soil parameters have been also added as they are indispensable for assessing soil fertility and health (Sousa et al., 2020). Research indicates that parameters such as bulk density (BDOD), cation exchange capacity (CEC), and sand and silt contents are crucial for understanding soil fertility, structure, and nutrient-holding capacity, which directly affects crop growth and yield (Yakubu et al., 2021). Furthermore, the presence of soil organic carbon (SOC) and nitrogen in the soil is indicative of soil health and fertility, which impacts plant growth and productivity (Salo et al., 2023). Thus, the selected parameters provide a comprehensive understanding of soil conditions crucial for optimal agricultural practices. All climate, soil, and fertiliser data were compiled by overlaying the yield dataset with spatial layers from global datasets. We first divide the global map into a raster of 0.1–0.1 °, which are 6480,000 in total, and collect data for each relevant cell. In terms of data, we use the sources mentioned in Table S1 in the supplementary information (SI).

2.1.2. Method

The supervised machine learning algorithm XGBoost (XGB) has been used to analyze the relationships between the independent variables and the explanatory variable. For example, the study of Li et al. (2023) used it to derive the relationship between crop yield and climate and soil. Also, He et al. (2024) used the same method to upscale local data by predicting the soil moisture content at a regional level based on field data. Unlike the Random Forest (RF) method, which builds trees independently using bootstrapped samples, the XGB machine-learning algorithm is based on gradient boosting by constructing an ensemble of decision trees in a sequential manner (Noorunnahar et al., 2023). Herein, each tree is built to address and correct the errors of the previous trees. The XGB method was applied to each crop individually. Here, we use the XGB implemented in the *xgboost* library from the Python *scikit-learn* module to perform the XGB regressions (Pedregosa et al., 2011).

The relevant calculations with the machine learning algorithm were carried out with Python 3.11. The hyperparameter *subsample, n_estimators, min_child_weight, max_depth, learning_rate,* and *colsample_bytree* were optimized using RandomizedSearchCV (scikit-learn version 1.2.2) between the input variables (soil, climate, and fertilizer parameters) and the output variable for each crop. In the optimization process, RandomizedSearchCV executed 20 iterations to maximize the R-squared value. A 3-fold cross-validation was also carried out to evaluate the XGB model, test it for each crop yield prediction and ensure robustness against overfitting. The model shows strong resistance to overfitting as the R-squared values for the training and test sets are consistently very close. For eucalyptus, the R-squared difference between training and test was 0.03, for miscanthus 0.01 and for poplar 0.02. Compared to other studies, the achieved R-squared values (0.73 for Eucalyptus, 0.69 for miscanthus, and 0.72 for poplar) are relatively high, which demonstrates the model's reliability. The mean absolute error (MAE) is also relatively low (3.17 for Eucalyptus, 4.37 for miscanthus, and 2.04 for poplar) compared to the mean value of 15.22 for eucalyptus, 12.5 for miscanthus, and 8.03 for poplar in the studies of (Anderson and Lucas, 2018; Fernández-Delgado et al., 2019; Hengl et al., 2017). The full set of optimized hyperparameters for each biomass, along with the R^2 values for training and test, as well as the MAE, is included in Table S3.

After training by data, the derived XBG model was used to predict the global distribution of the lignocellulosic crop yields. Herein, three predictions were made, one for each individual prescribed lignocellulosic crop. Although lignocellulosic crops are very drought- and cold-tolerant, most species still have a cold and water limit (Zhao et al., 2021). Also, because XGB models have poor ability to extrapolate when the values of explanatory variables are outside the ranges of training data, we only limited each crop prediction to the areas that are adequate for growth. Specifically, the minimum mean temperature and precipitation over all grid cells in the training dataset were derived for each crop. The regions adequate for growth of each lignocellulosic crop were then defined as grid cells with mean temperature and precipitation higher than the maximums in the datasets. In other words, if either mean temperature or precipitation in a grid cell is lower than the minimums in the training data, this grid cell is excluded for this crop. This way, the dataset decreased from 1386,000 grid cells to 428,102 for eucalyptus, 560,408 for miscanthus, and 839,218 for poplar. The minimum mean temperature and precipitation as well as the number of grid cells for each crop are shown in Table S2. The results of the three crops are then integrated into QGIS to visualize the outcomes.

2.2. Biomass production cost

2.2.1. Data

After estimating the potential global yield of three selected lignocellulosic crops, the associated roadside costs for each crop were subsequently calculated. Roadside costs encompass the expenses incurred from initial soil preparation prior to sowing through to the transportation of harvested biomass to roadside collection points. This includes crop establishment, fertilizing, crop protection, harvesting/cuttings, uprooting, baling, shredding, chipping, crushing, collecting, and densifying at the point of harvest. To do so, an extensive inventory was compiled to collect the relevant costs and prices, i.e. irrigation, labor, electricity, fuel, gas, and LPG, fertilizer and pesticides. Irrigation costs are based on the work of Caldera and Breyer (2020), who developed a country-specific database for irrigation costs. According to their study, irrigation costs depend on the type of irrigation system, access to saline water for desalination, and the costs of renewable energy for either desalinating seawater or pumping groundwater. However, following Dees et al. (2017) and Panoutsou and Chiaramonti (2020), it is assumed that the required irrigation depends on local precipitation. Minimum water requirements for miscanthus and eucalyptus are set at 500 mm and for poplar at 600 mm (Dees et al., 2017), calculated from the combination of precipitation (chapter 2.1.2) and irrigation. Therefore, if precipitation at a given location exceeds these thresholds, no irrigation costs are calculated.

Labor costs are based on the database developed by ILOSTAT (2024) for *statutory nominal gross minimum wage*, which records the minimum wages in each country. The minimum wage was selected as a reference because it is considered representative of agricultural labor, as noted by Kandilov and Kandilov (2020). However, since the database (ILOSTAT, 2024) is incomplete, minimum wage values

were estimated to fill data gaps. Herein, a linear correlation between minimum wage and GDP per capita was performed based on the database of World Bank Group (2024), as shown in Figure S1. With R-squared of 0.659, a linear relationship between GDP per capita and minimum wage in USD was established, as expressed in Eq. (1). Due to potential inconsistencies between (ILOSTAT, 2024) minimum wage data and acutal wages in some countries, Eq. 1 was applied consistently across all countries. For the prices of electricity, diesel, gas, and LPG, the database of globalpetrolprices (2024) was used. Among 197 countries worldwide, 147 entries for electricity, 53 for LPG, 48 for natural gas, and 168 for diesel were available. For countries lacking data entries, the global median value was used. As fertilizer and pesticides are globally traded commodities, a uniform global value for each was adopted based on (FAO, 2024).

$$Y = 0.028*x + 48.693 \quad (1)$$

2.2.2. Cost modelling for biomass production

For this study, two distinct cost models were developed: one specific to miscanthus assuming a plantation lifetime of 15 years and another for eucalyptus and poplar assuming a plantation lifetime of 12 years each (Cintas et al., 2021). Herein, it is assumed that all of them share the same cost structure associated with woody biomass crops (Cintas et al., 2021). Since the primary incentive to cultivate bioenergy crops is to contribute to more sustainability, it is necessary to constrain the bioenergy cultivation on marginal land to avoid conflicts with existing forests and diverting land resources from food production. In this study, we determined only bare ground of terra firma (which means solid ground) and wetland based on the global land cover and land use 2019 map developed by Hansen et al. (2022). This includes savannas, shrubland, and grassland as marginal lands. The global map was downloaded separately with 283 pieces. All land use types except bare ground on terra firma and wetland were excluded via QGIS 3.36. The cost of marginal land is neglected as all the three crops are assumed to be grown on marginal land without alternative economic use (Cintas et al., 2021; Dees et al., 2017). The detailed assumptions for the cost models as well as the calculations are included in SI. The cost model for eucalyptus and poplar is based on (Romanelli et al., 2008) (Table S6) and the cost model for miscanthus is based on Panoutsou and Chiaramonti (2020) (Table S7), including labor time, resource consumption, machinery time and type. The fuel consumption and machinery cost per hour is based on (Dees et al., 2017; Panoutsou and Chiaramonti, 2020) as seen in Table S8.

2.3. Transportation cost

The transport cost between cropland and the pyrolysis plant is influenced by three main factors: processing capacity, spatial distribution and density of available biomass, and local transport accessibility (Han et al., 2022). In this study, transport costs were estimated by determining the average service distance required to meet the biomass demand of plant. This distance depends on both the biomass availability in the surrounding area and the plant's capacity, which vary across the different scenarios considered. The analysis was conducted on a global grid with a resolution of $0.1^\circ \times 0.1^\circ$. To calculate intercellular distances between each potential biomass source and the central pyrolysis facility, the Haversine formula was used. All distances were then adjusted by a detour factor of 1.3 to reflect realistic transport routes and road networks (Lee and Moon, 2024). For transportation within the grid cells, a separate approach was applied. For smaller-capacity systems, sufficient biomass is typically available within the same cell, making intercell transport unnecessary. To estimate intra-cell distances, we used an analytical approximation of the mean Euclidean distance from randomly distributed points within a square to its center, expressed as $L / \sqrt{6}$, where L is the cell length. This average was then multiplied by a detour factor of 1.3 to reflect real-world deviations from straight-line movement within each grid cell.

2.4. Pyrolysis costs

There is a wide range of technologies for biochar production. Pyrolysis systems with high technological standards are characterized by high automatization, low emission levels and the capability to produce heat and electricity through efficient utilization of process heat (Azzi et al., 2022; Letoffet et al., 2024; Zhou et al., 2020). For example, Pyreg develops a mature pyrolysis unit equipped with an after-combustion chamber with the ability to use district heat (Azzi et al., 2022; Sørmo et al., 2020). However, such pyrolysis systems require permanent electricity and gas infrastructure. Thus, low-tech alternatives are also used where those conditions are not available (Cornelissen et al., 2023; Namaswa et al., 2023). Pyrolysis systems with low technological standards are characterized by being independent of electricity and gas infrastructure as it only needs the oven materials (i.e. steel) (Cornelissen et al., 2023; Karananidi et al., 2020; Namaswa et al., 2023; Pandit et al., 2017). The three most widely used technologies are retort kilns (Adeniyi et al., 2023; Ighalo et al., 2022; Kafkova, 2021), top-lit up-draft (TLUD) (Howell et al., 2021) and the Kontiki flame curtain kiln (Karananidi et al., 2020). Due to the high greenhouse gas process emissions and higher biochar production costs of retort kilns and TLUD systems, the Kontiki flame curtain kiln was selected for the analyses (Kafkova, 2021; Smebye et al., 2017). However, the scalability of Kontiki systems was not considered in this study, as they are inherently limited by safety-related constraints and manual operation, which restrict their applicability in large-scale settings.

A comprehensive spreadsheet-based model is developed to evaluate the economic performance of the biochar production system of both technological pathways (i.e. Pyreg plant and Kontiki flame curtain kiln). We examine how the number and location of processing sites affect capital costs (CAPEX), operational costs (OPEX), and transportation expenses. The equipment purchase cost is sourced from the machine PX1500 by Pyreg company, with an annual feedstock consumption of 3300 tons (PYREG, 2024). A scale factor of 0.6 is

used for scaling calculations (Tribe and Alpine, 1986). OPEX is calculated based on both CAPEX and product sales. Annual CAPEX is estimated over a 20-year plant lifespan with a discount rate of 5 %. The key assumptions for the techno-economic analysis (TEA) for both the Kontiki flame curtain kiln and the Pyreg plant are summarized in Table 1. The cost benefits of syngas and excess heat from the Pyreg plants are excluded in the base case (Tang et al., 2024). The assumptions for the Kontiki flame curtain kiln are based on the life cycle inventories developed by Smebye et al. (2017) and Namaswa et al. (2023). The biochar-to-biomass ratio for each of the three biomasses is calculated following Azzi et al. (2022). The assumptions and the biochar-to-biomass ratios are provided in Table S5, based on (Azzi et al., 2022; Daniel et al., 2018; Ruett et al., 2024; Wallikhani et al., 2022).

3. Results & discussion

3.1. Global distribution of biochar production cost

The results show that the biochar production cost range between 113.36 and 1548.85 €/ton, depending on the technology, scale, biomass and region. Fig. 2 shows the lowest production cost achieved with the Kontiki flame curtain kiln and indicate the biomass with lowest value. Fig. 3 depicts the results of the Pyreg plant with a capacity of 100,000 tons of biochar output per year, without the use of district heat. For the detailed results, the distribution of the production cost for each biomass, technology and Pyreg plant size are included in Figures S3-S6. For both technologies, the biochar of eucalyptus is the cheapest in most of the parts in South America and Africa, as well as in Southeast Asia. Poplar has the lowest production costs mainly in Central and West Asia, Northwest America, Central Australia and Northern Europe, whereas biochar of Miscanthus is the cheapest in parts of Europe, North America, Australia and Eastern Africa. In a total of 833,339 data points, biochar from eucalyptus is the cheapest for 409,386 data points for the Kontiki flame curtain kiln and for 418,973 data points for the Pyreg plant. Biochar from poplar was the cheapest for 351,090 data points for the Kontiki flame curtain kiln and for 300,271 data points for the Pyreg plant. Biochar from poplar was the cheapest for 72,863 data points for the Kontiki flame curtain kiln and for 111,095 data points for the Pyreg plant.

In terms of production costs, both technologies show lower production costs for biochar in Sub-Saharan Africa, Latin America & Caribbean and South Asia compared to Oceania, North America, Europe and North and East Asia. Figure S7 shows the division of the globe into regions. According to this division, the minimum, maximum and median costs per region are shown in Table 2 and the distribution is shown in Fig. 4. Sub-Saharan Africa consistently shows the lowest production costs across both technologies, with median values of 197.82 €/ton for the Kontiki flame curtain kiln and 290.21 €/ton for the Pyreg plant, making it the most cost-effective region. Latin America, Caribbean and South Asia follow with similarly low median costs, below 300 €/ton for both technologies. These regions benefit from low feedstock prices and low labor costs, making them highly suitable for decentralized and low-cost biochar production. Herein, similar regional trends have been observed in broader reviews of biochar economics, which highlight lower feedstock and labor prices as the primary determinants of low-cost production in the Global South (Campion et al., 2023; Owsianiak et al., 2021; Torres-Morales et al., 2023).

In contrast, Oceania, North America, and Europe report the highest median production costs. For instance, in Oceania, the median cost reaches 899.48 €/ton for the Kontiki flame curtain kiln and 566.94 €/ton for the Pyreg plant, driven by high operational expenditures. North America also shows elevated values with a median cost of 880.90 €/ton for the Kontiki flame curtain kiln and 630.87 €/ton for the Pyreg plant. These cost levels reflect higher labor costs, and more expensive biomass and energy inputs. Comparable cost levels in developed markets were also reported by Bergman et al. (2022) and Sahoo et al. (2019), emphasizing that energy and labor inputs dominate cost composition in high-income regions. Interestingly, the Pyreg plant tends to exhibit a narrower cost range between the maximum and minimum costs and generally lower median costs than the Kontiki flame curtain kiln in high-income regions such as East Asia and Europe. This indicates that larger-scale and high-tech systems might benefit from better efficiencies in well-developed

Table 1
Parameters and assumptions considered for cost assessment for the Kontiki flame curtain kiln and Pyreg plants.

Category	Parameter	Kontiki flame curtain kiln	Pyreg PX1500 plant
System lifespan	Lifespan (reused runs / years)	500 runs (Smebye et al., 2017)	20 years (PYREG, 2024)
Capital cost	Core equipment	Steel (80 kg), welding steel (10 m) (Smebye et al., 2017)	Pyrolyses plant: 2000,000€ (PYREG, 2024)
	Auxiliary equipment	-	Dryer/shredder: 300,000€; Pelletizer: 50,000€ (PYREG, 2024)
	Production time	2 h	-
Fixed OPEX	Labor	24.23 h/t (Namaswa et al., 2023)	1333 h/a (PYREG, 2024)
	Insurance	-	0.5 % of CAPEX (PYREG, 2024)
	Maintenance	-	2.5 % of CAPEX (PYREG, 2024)
	Land rent	-	215 m^2 (PYREG, 2024)
Operational OPEX	Water use	334 kg/t biochar	160 m^3/a (PYREG, 2024)
	Energy use	-	288 MWh/a (PYREG, 2024)
	Fuel (LPG)	-	9400 l/a (PYREG, 2024)
Scale factor	For CAPEX scaling	-	0.6 (Tribe and Alpine, 1986)
Discount rate	For CAPEX amortization	-	5 % (Tang et al., 2024)

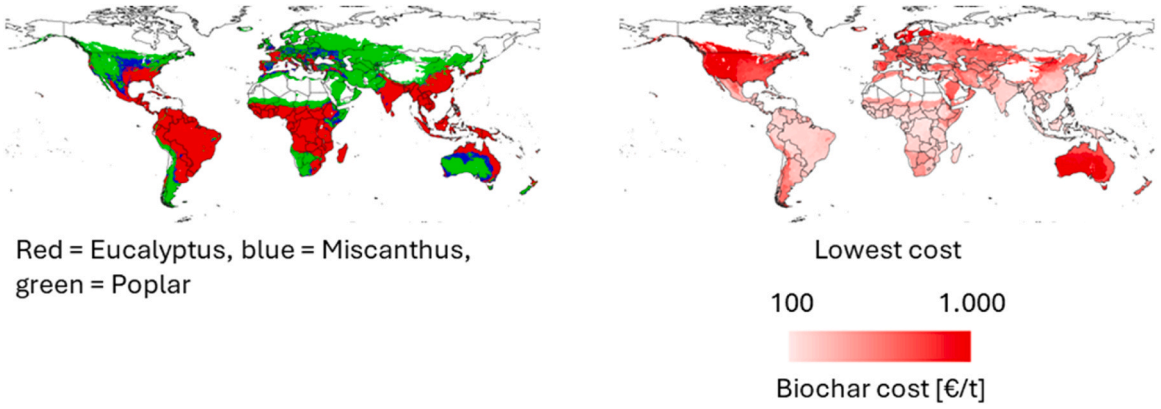

Fig. 2. Biochar production cost with the Kontiki flame curtain kiln showing the biomass with the lowest production cost (left) and the lowest cost by region (right).

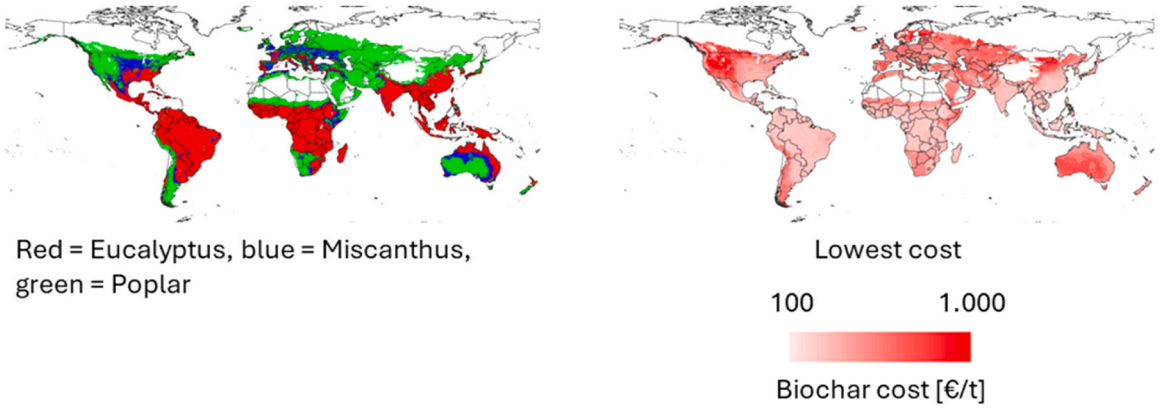

Fig. 3. Biochar production cost with Pyreg plant with a capacity of 100.000 tons of biochar per year without the use of district heat showing the biomass with the lowest production cost (left) and the lowest cost by region (right).

Table 2
Minimum, maximum and median production cost per region in €/ton shown in Figure S7.

Region	Kontiki flame curtain kiln			Pyreg plant with a capacity of 100,000 ton of biochar output per year without district heat		
	Min cost	Max cost	Median cost	Min cost	Max cost	Median cost
East Asia	128.24	1525.47	667.52	206.43	1091.52	375.27
Europe	292.10	1548.85	547.85	299.90	1268.66	497.61
Latin America & Caribbean	138.61	688.12	221.13	208.13	664.59	268.53
Middle East & North Africa	216.79	845.00	499.48	258.31	770.82	474.93
North America	549.90	1275.46	880.90	317.16	1004.00	630.87
South Asia	129.96	661.49	210.77	202.22	703.98	287.03
Sub-Saharan Africa	113.36	531.97	197.82	201.54	593.85	290.21
North Asia	301.19	957.86	604.53	317.45	908.93	582.21
Oceania	607.58	1068.61	899.48	354.28	775.64	566.94

markets. However, in lower-cost regions like South Asia or Africa, the Kontiki flame curtain kiln remains the most cost-efficient option, due to its simplicity and lower upfront investments.

3.2. District heat

Furthermore, the Pyreg plant has the capacity to generate district heat (PYREG, 2024). The heat potential is calculated per biomass type based on the assumptions provided by the study of Azzi et al. (2022), which estimates the energy content of the excess heat generated during the pyrolysis process. It is assumed that this heat is directly used by a nearby industrial or municipal facility and

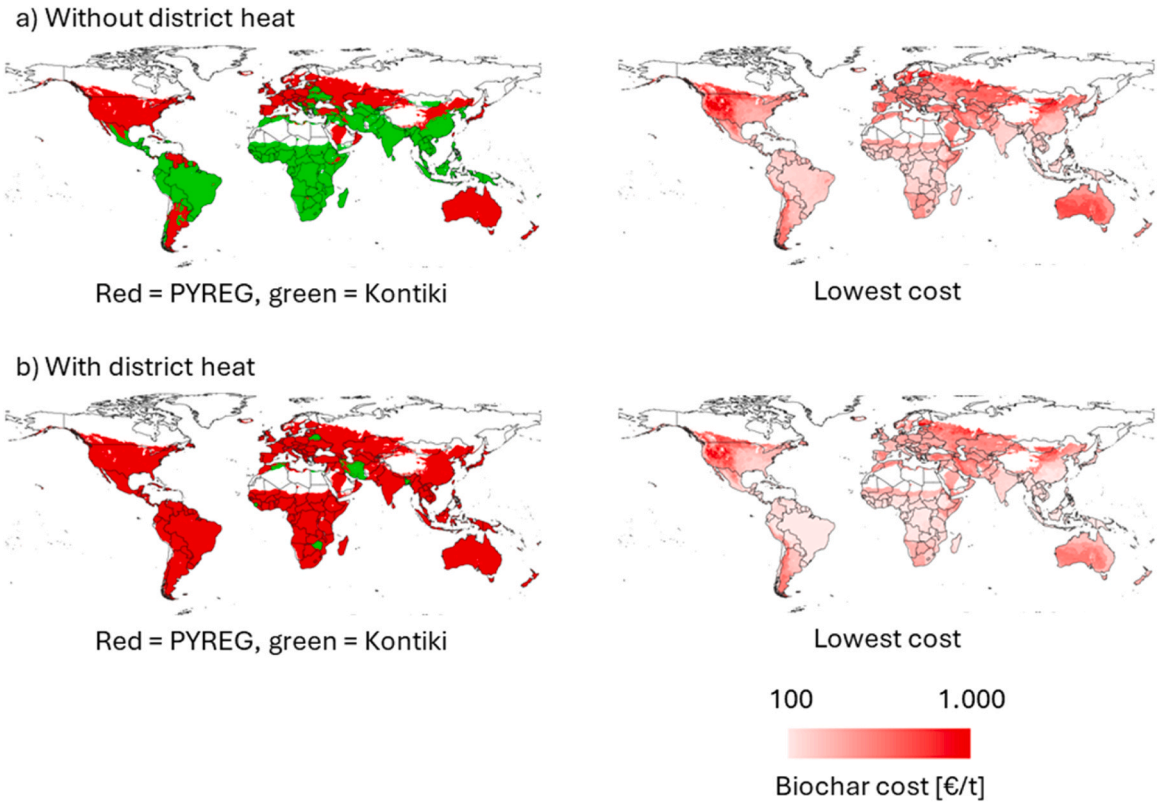

Fig. 4. Biochar production cost comparing the Kontiki flame curtain kiln with Pyreg plant with a capacity of 100,000 tons of biochar per year without district heat (a) and with district heat (b).

replaces a conventional natural gas-fired heat boiler. Following Klaassen and Patel (2013), a boiler efficiency of 0.95 and region-specific natural gas prices are applied to estimate the monetary value of the recovered heat. Previous LCA and TEA studies similarly emphasize that heat valorization can reduce net production costs, especially in combined heat and biochar systems (Bergman et al., 2022; Sahoo et al., 2019). Herein, the integration of district heat revenues significantly changes the economic feasibility of the Pyreg plant. Fig. 4 illustrates the global comparison of optimal technology when district heat use is taken into account. In contrast to the previous comparison, the Pyreg plant now emerges as the more cost-effective technology across almost all regions. This is particularly true in Europe, North America, East Asia, and parts of Central Asia, where high natural gas prices and developed infrastructure make heat substitution highly valuable.

However, there are notable exceptions in the other regions. Despite the available heat from Pyreg, the Kontiki flame curtain kilns are more cost-effective in countries such as Iran, Zimbabwe, Algeria, and Belarus. The reason lies in the low natural gas prices in these countries, which significantly reduce the economic benefit of substituting natural gas with district heat. As a result, the additional capital and operational costs of the Pyreg plant are not compensated by sufficient heat revenues in these countries. Overall, Fig. 4 shows that when district heat can be efficiently utilized, Pyreg plants become the more attractive option globally, even in many lower-income regions. Nevertheless, it is important to consider that these results are based on the assumption of an existing market or infrastructure for district heat. In reality, such infrastructure might be absent, particularly in rural or less-developed regions, which may limit the applicability of these results. In regions without centralized heating networks or with low industrial heat demand, the simpler and more decentralized Kontiki flame curtain kilns may remain a more realistic and cost-effective choice.

3.3. Cost structure of biochar production cost

Fig. 5 show the average cost structure of biochar production across world regions for both technologies. The results reflect the cost distributions, based on median values per region. For the Pyreg plant, the largest share of production cost is driven by biomass costs, followed by energy costs and CAPEX. In regions where natural gas is expensive and district heating infrastructure exists, such as Europe, North Asia, and Oceania, revenues from selling excess heat can significantly lower total production costs. In contrast, in regions like Sub-Saharan Africa, South Asia, East Asia, and Latin America & the Caribbean, the benefit of heat recovery is minimal due to the lack of infrastructure. In these areas, low-tech solutions like the Kontiki flame curtain kiln remain the more cost-effective option, even without heat utilization, as shown in Fig. 4. The Kontiki flame curtain kiln shows a more labor-intensive cost structure. Biomass costs and labor costs are the dominant cost drivers, while CAPEX and water use contribute marginally. The system performs

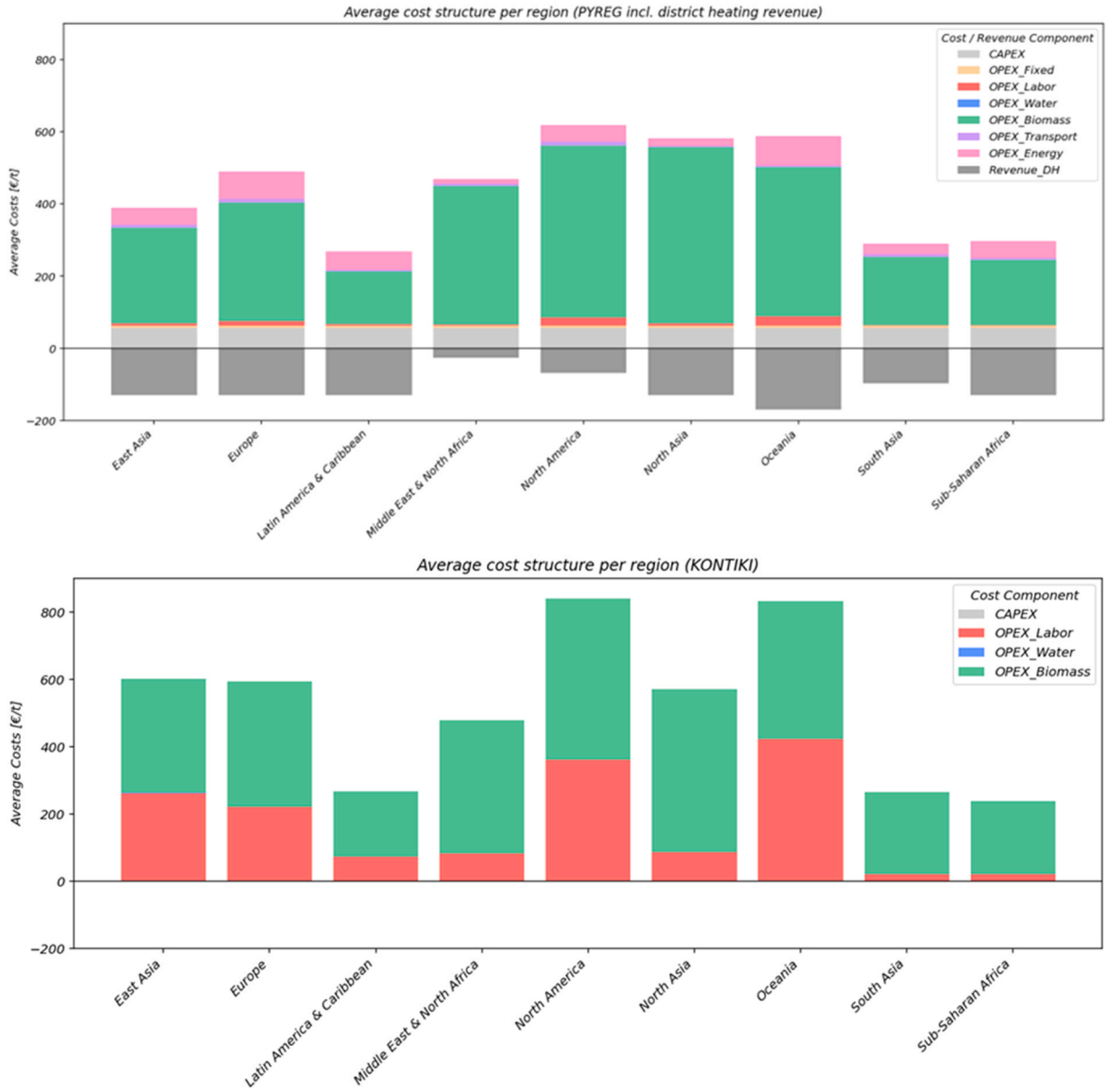

Fig. 5. Cost structure of Pyreg plant including district heat revenue and Kontiki flame curtain kiln. For the Kontiki flame curtain kiln, it should be noted that CAPEX and OPEX_Water are so small that they are difficult to see in the figure.

particularly well in regions with low biomass and labor costs, such as Sub-Saharan Africa and South Asia.

It is important to note that if the production capacity of the Kontiki flame curtain kiln could be increased while maintaining safety standards, labor costs would decrease significantly, improving its competitiveness compared to the Pyreg plant. This underlines the potential of process optimization and scaling even for low-tech systems. Regarding the Pyreg plant, the decisive factor for its cost-effectiveness is the utilization of district heat, as shown by the change in Fig. 4. Finally, the results show that transportation costs have only a minor impact on total production costs in both systems. When compared to CAPEX, their contribution is negligible. This observation aligns with the analyses of Bergman et al. (2022) and Sahoo et al. (2019), which highlight that transport logistics contribute less than 10 % to total costs, whereas CAPEX and energy remain dominant drivers. This suggests that future research and development should focus on developing larger, scalable Pyreg plant units with lower CAPEX. Current estimates are based on upscaling and not on fully engineered large-scale designs, leaving room for future efficiency gains.

3.4. Validation

The global distribution of biomass production costs for eucalyptus, miscanthus, and poplar is illustrated in Figure S2. The results have been validated by comparing the results with the analyses of earlier studies. The study by Dees et al. (2017) provides biomass roadside cost estimates for various feedstocks, including forestry residues, agricultural residues, secondary industrial residues, and lignocellulosic biomass (e.g., eucalyptus), at regional and national levels. Fig. 6 presents a comparison between the eucalyptus cost estimates derived in this study and those reported by the S2BIOM database (Dees et al., 2017; S2BIOM, 2012), adjusted using the producer price index for the period 2015–2023 (EUROSTAT, 2024). On average, the absolute deviation in cost estimates by country amounts to 39 %. The largest discrepancies are observed in Bosnia (89.18 %), Kosovo (84.52 %), and Luxembourg (69.03 %). These differences are primarily attributable to the limited granularity of the S2BIOM dataset, which in some cases includes only a single data point per country. In contrast, countries with a higher number of recorded entries show substantially lower deviations. For example, Germany (402 entries) shows a deviation of only 5.76 %, followed by France (96 entries, 4.44 %), the United Kingdom (173 entries, 12.74 %), Italy (110 entries, 17.38 %), and Spain (59 entries, 28.95 %).

4. Conclusion & outlook

The study presents a comprehensive techno-economic framework to estimate the production costs of biochar using various lignocellulosic biomass sources and processes at a global level. The proposed approach is essential to optimize local and global biomass utilization pathways, including the unexplored potential of marginal lands. By combining machine learning-based yield prediction, cost modeling for biomass cultivation and harvesting, and the analysis of two pyrolysis technologies, the study identifies spatially explicit cost structures under varying regional and technological conditions. Thus, the study contributes to the strategic understanding of global biochar cost structures and provides a data-driven foundation to support decision-making. The presented analyses are also crucial for optimizing global CDR strategies, which depend on accurate predictions across emerging CDR technologies and applications. Accurate cost forecasting for each technology is critical for identifying the most cost-effective mix of technologies. Additionally, optimizing biochar supply chains on a global scale can help in pinpointing low-cost biochar production sites, supporting the development of future markets.

The outcomes underscore the importance of aligning biochar production strategies with regional conditions, infrastructure availability, and technological capabilities. While biochar has promising potential within global climate mitigation portfolios, its feasibility remains highly context-specific, which requires tailored, spatially explicit approaches to unlock its full potential. The results reveal substantial regional differences in terms of biochar production costs. The lowest median costs are observed in Sub-Saharan Africa, Latin America & Caribbean, and South Asia, primarily due to favorable climatic conditions, high biomass yields, and low labor costs. Eucalyptus-based biochar emerges as the most cost-effective option in most regions. In contrast, developed regions such as Europe, North America, and Oceania show significantly higher production costs, driven by increased input prices and operational expenditures. A key insight is that low-tech systems like the Kontiki flame curtain kiln are especially well-suited for decentralized and low-income contexts. On the other hand, high-tech systems such as Pyreg plants gain economic competitiveness in industrialized regions, particularly when excess heat can be monetized. The inclusion of district heat as a scenario demonstrates the potential economic advantage of this option, while acknowledging that the required infrastructure is often unavailable or underdeveloped in many parts of the world.

From a practical perspective, the spatially explicit cost maps provide actionable guidance for stakeholders. First, they enable policy makers and investors to prioritize near-term deployment in regions with low median costs (e.g., $<$300 €/ton in Sub-Saharan Africa, Latin America & Caribbean, and South Asia). Second, they support context-driven technology decisions, favoring decentralized, low-tech systems in low-infrastructure settings and high-tech plants in industrialized regions where excess heat can be used. Third, they inform infrastructure and market planning by quantifying the value of district-heat integration and identifying geographic high-potential areas for subsequent high-resolution siting, logistics, and market studies.

Although the study strived for the highest level of accuracy, it is still subject to some limitations due to data availability. First, the global datasets on biomass availability, wage levels, energy prices, and input costs are sometimes incomplete or inconsistent across regions. Consequently, median values and estimation formulas were used, which may impact the accuracy in data-scarce regions. In addition, seasonal variations in biomass properties (e.g., moisture and ash content) were not explicitly modeled, although their influence on the key findings is expected to remain minor at the aggregated global scale. Second, the techno-economic analysis relies on globally uniform assumptions and does not reflect country-specific financing conditions, subsidies, or investment risks. Third, the analysis is static and does not incorporate dynamic developments such as policy changes, market trends, or technological learning curves. In terms of spatial resolution, although the 0.1° grid (~11 km) provides a useful global overview, it cannot capture micro-regional characteristics such as slope, access routes, or land-use conflicts. Furthermore, the classification of marginal lands is based on land cover data and does not include deeper considerations of land tenure, biodiversity risks, or socio-ecological constraints.

Looking forward, several areas offer opportunities for extending the presented approach. Future research could incorporate Life Cycle Assessment to assess the full environmental performance of biochar production under varying conditions. This includes the consideration of potential land-use changes following the cultivation of marginal lands, which were not included in this study due to its exclusive economic focus. Addressing this aspect in environmental assessments would allow for a more holistic understanding of sustainability trade-offs. The integration of policy scenarios, such as regional carbon prices or subsidy schemes, would improve the relevance of cost forecasts, although such modeling remains methodologically demanding due to the diversity of national frameworks. Additionally, while transport costs had only a minor impact on total costs in this study, refining the transport modeling through the

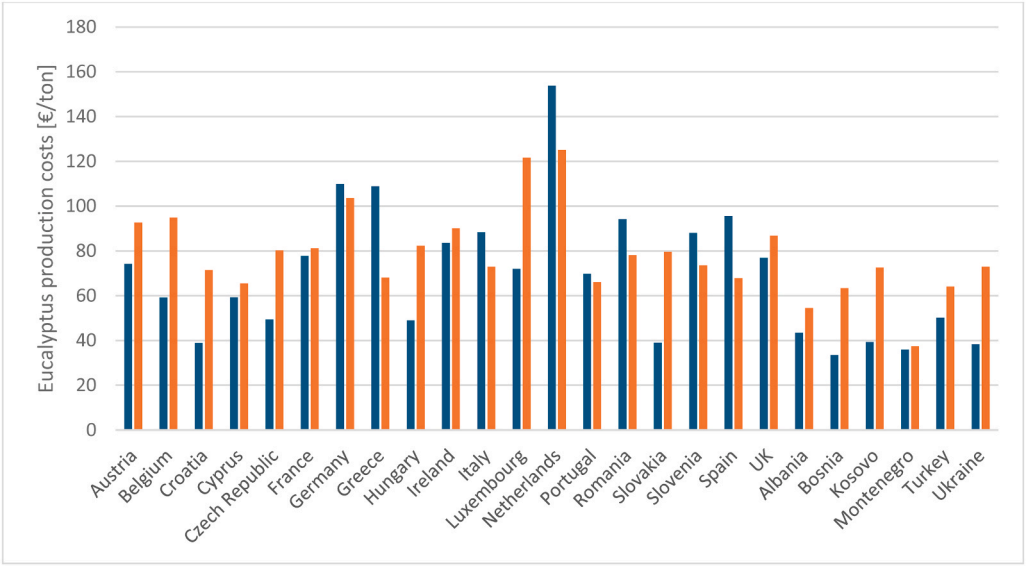

Fig. 6. Validation – comparison of total eucalyptus production costs between own results and S2BIOM project at a national level in Europe.

inclusion of real road networks and infrastructure accessibility could benefit site-specific applications. Furthermore, a promising research avenue is to link production-side cost modeling with downstream market applications to identify which biochar end uses, such as soil amendment, carbon trading, or industrial feedstocks, offer the highest economic value under different regional conditions. Another important avenue is the development of dynamic cost models that can project future production costs under changing technological, economic, and political conditions. This includes learning effects, economies of scale, and shifts in biomass market availability. Such models could help identify long-term investment strategies and policy levers to foster biochar deployment.

CRediT authorship contribution statement

Kern Johannes Jakob: Writing – original draft, Visualization, Validation, Software, Methodology, Investigation, Formal analysis, Data curation, Conceptualization. **Ali Abdelshafy:** Writing – review & editing, Supervision, Conceptualization. **Grit Walther:** Writing – review & editing.

Declaration of Competing Interest

The authors declare the following financial interests/personal relationships which may be considered as potential competing interests: In addition to his scientific work at RWTH Aachen University, Mr. Johannes Kern is co-founder of the start-up RecyCoal. RecyCoal develops biochar carbon removal projects in Rwanda, Tanzania, and Senegal. General expertise in the field have contributed to the models used in this work; however, the start-up's interests did not influence the contents, methods of evaluation, or conclusions of the paper. If there are other authors, they declare that they have no known competing financial interests or personal relationships that could have appeared to influence the work reported in this paper.

Appendix A. Supporting information

Supplementary data associated with this article can be found in the online version at doi:10.1016/j.eti.2025.104658.

Data availability

Data will be made available on request.

References

Adeniyi, A.G., Iwuozor, K.O., Adeleke, J., Emenike, E.C., Micheal, K.T., Ighalo, J.O., 2023. Production and characterization of neem leaves biochar: effect of two different retort carbonization systems. Bioresour. Technol. Rep. 24, 101597. https://doi.org/10.1016/j.biteb.2023.101597.

Adhikari, S., Moon, E., Paz-Ferreiro, J., Timms, W., 2024. Comparative analysis of biochar carbon stability methods and implications for carbon credits. Sci. Total Environ. 914, 169607. https://doi.org/10.1016/j.scitotenv.2023.169607.

Anderson, G.J., Lucas, D.D., 2018. Mach. Learn. Predict. a Multiresolution Clim. Model Ensemble.
Azzi, E.S. [Elias S.], Karltun, E., Sundberg, C., 2021. Assessing the diverse environmental effects of biochar systems: an evaluation framework. J. Environ. Manag. 286, 112154. https://doi.org/10.1016/j.jenvman.2021.112154.
Azzi, E.S. [Elias S.], Karltun, E., & Sundberg, C. (2022). Life cycle assessment of urban uses of biochar and case study in Uppsala, Sweden, *2022*. ⟨https://link.springer.com/article/10.1007/s42773-022-00144-3⟩.
Batjes, N.H. (2020). *Soilgrids.* ISRIC World Soil Information. ⟨https://www.isric.org/⟩.
Bergman, R., Sahoo, K., Englund, K., Mousavi-Avval, S.H., 2022. Lifecycle assessment and techno-economic analysis of biochar pellet production from forest residues and field application. Energies 15 (4), 1559. https://doi.org/10.3390/en15041559.
Breunig, H.M., Rosner, F., Lim, T.-H., Peng, P., 2023. Emerging concepts in intermediate carbon dioxide emplacement to support carbon dioxide removal. Energy Environ. Sci. 16 (5), 1821–1837. https://doi.org/10.1039/D2EE03623A.
Caldera, U., Breyer, C., 2020. Strengthening the global water supply through a decarbonised global desalination sector and improved irrigation systems. Energy 200, 117507. https://doi.org/10.1016/j.energy.2020.117507.
Campion, L., Bekchanova, M., Malina, R., Kuppens, T., 2023. The costs and benefits of biochar production and use: a systematic review. J. Clean. Prod. 408, 137138. https://doi.org/10.1016/j.jclepro.2023.137138.
Cintas, O., Berndes, G., Englund, O., & Johnsson, F. (2021). Geospatial supply-demand modeling of lignocellulosic biomass for electricity and biofuels in the European Union. ⟨https://www.sciencedirect.com/science/article/pii/S0961953420304049⟩.
Cornelissen, G., Sørmo, E., La Rosa, R.K.A. de, Ladd, B., 2023. Flame curtain kilns produce biochar from dry biomass with minimal methane emissions. Sci. Total Environ. 903, 166547. https://doi.org/10.1016/j.scitotenv.2023.166547.
Daniel, D.J., Ellison, C.R., Bursavich, J., Benbow, M., Favrot, C., Blazier, M.A., Marculescu, C., Nokes, S.E., Boldor, D., 2018. An evaluative comparison of lignocellulosic pyrolysis products derived from various parts of Populus deltoides trees and Panicum virgatum grass in an inductively heated reactor. Energy Convers. Manag. 171, 710–720. https://doi.org/10.1016/j.enconman.2018.06.026.
Dees, M., Höhl, M., Datta, P., Forsell, N., Leduc, S., Fitzgerald, J., Verkerk, H., Zudin, S., Lindner, M., Elbersen, B., Staritzky, I., Schrijver, R., Lesschen, J.-P., van Diepen, K., Anttila, P., Prinz, R., Ramirez-Almeyda, J., Monti, A., Vis, M., … Glavonjic, B. (2017). A spatial data base on sustainable biomass cost-supply of lignocellulosic biomass in Europe - methods & data sources.
Ehsan, F., Habib, S., Gulzar, M.M., Guo, J., Muyeen, S.M., Kamwa, I., 2024. Assessing policy influence on electric vehicle adoption in China: An in-depth study. Energy Strategy Rev. 54, 101471. https://doi.org/10.1016/j.esr.2024.101471.
EUROSTAT. (2024). *Industrial producer price index overview.* ⟨https://ec.europa.eu/eurostat/statistics-explained/index.php?title=Industrial_producer_price_index_overview#Data_sources⟩.
FAO, 2024. Food Outlook – Biannual Report on Global Food Markets. FAO. https://doi.org/10.4060/cd1158en.
Fernández-Delgado, Sirsat, Cernadas, Alawadi, Barro, & Febrero-Bande (2019). An extensive experimental survey of regression methods.
Fuss, S., Lamb, W.F., Callaghan, M.W., Hilaire, J., Creutzig, F., Amann, T., Beringer, T., Oliveira Garcia, W. de, Hartmann, J., Khanna, T., Luderer, G., Nemet, G.F., Rogelj, J., Smith, P., Vicente, J.L.V., Wilcox, J., Del Mar Zamora Dominguez, M., Minx, J.C., 2018. Negative emissions—Part 2: costs, potentials and side effects. Environ. Res. Lett. 13 (6), 63002. https://doi.org/10.1088/1748-9326/aabf9f.
globalpetrolprices. (2024). *Retail energy price data.* ⟨https://www.globalpetrolprices.com/⟩.
Grigorieva, E., 2020. Evaluating the sensitivity of growing degree days as an agro-climatic indicator of the climate change impact: a case study of the Russian Far East. Atmosphere 11 (4), 404. https://doi.org/10.3390/atmos11040404.
Han, M., Zhao, Q., Li, W., Ciais, P., Wang, Y.-P., Goll, D.S., Zhu, L., Zhao, Z., Wang, J., Wei, Y., Wu, F. [Fengchang], 2022. Global soil organic carbon changes and economic revenues with biochar application. GCB Bioenergy 14 (3), 364–377. https://doi.org/10.1111/gcbb.12915.
Hansen, M.C., Potapov, P.V., Pickens, A.H., Tyukavina, A., Hernandez-Serna, A., Zalles, V., Turubanova, S., Kommareddy, I., Stehman, S.V., Song, X.-P., Kommareddy, A., 2022. Global land use extent and dispersion within natural land cover using Landsat data. Environ. Res. Lett. 17 (3), 34050. https://doi.org/10.1088/1748-9326/ac46ec.
He, S., Zhou, L., Xie, H., Tan, S., 2024. Enhancing XGBoost's accuracy in soil organic matter prediction through feature fusion. Paddy Water Environ. 22 (3), 475–489. https://doi.org/10.1007/s10333-024-00980-y.
Hengl, T., Mendes de Jesus, J., Heuvelink, G.B.M., Ruiperez Gonzalez, M., Kilibarda, M., Blagotić, A., Shangguan, W., Wright, M.N., Geng, X., Bauer-Marschallinger, B., Guevara, M.A., Vargas, R., MacMillan, R.A., Batjes, N.H., Leenaars, J.G.B., Ribeiro, E., Wheeler, I., Mantel, S., Kempen, B., 2017. Soilgrids250m: Global gridded soil information based on machine learning. PloS One 12 (2), e0169748. https://doi.org/10.1371/journal.pone.0169748.
Howell, N., Pimentel, A., Bhattacharia, S., 2021. Material properties and environmental potential of developing world-derived biochar made from common crop residues. Environ. Chall. 4, 100137. https://doi.org/10.1016/j.envc.2021.100137.
Ighalo, J.O., Eletta, O.A., Adeniyi, A.G., 2022. Biomass carbonisation in retort kilns: Process techniques, product quality and future perspectives. Bioresour. Technol. Rep. 17, 100934. https://doi.org/10.1016/j.biteb.2021.100934.
ILOSTAT. (2024). *Statutory nominal gross monthly minimum wage.* ⟨https://rshiny.ilo.org/dataexplorer54/?lang=en&id=EAR_4MMN_CUR_NB_A⟩.
IPCC. (2023). *Climate Change 2022 – Impacts, Adaptation and Vulnerability: Working Group II Contribution to the Sixth Assessment Report of the Intergovernmental Panel on Climate Change*.
Ishikawa, S., Nakashima, T., Iizumi, T., Hare, M.C., 2020. Evaluating irrigated rice yields in Japan within the Climate Zonation Scheme of the Global Yield Gap Atlas. J. Agric. Sci. 158 (8-9), 718–729. https://doi.org/10.1017/S0021859621000186.
Kafkova, D. (2021). Life Cycle Assessment of biochar produced from waste wood in the durnace Kon-Tiki.
Kandilov, A.M.G., Kandilov, I.T., 2020. The minimum wage and seasonal employment: Evidence from the US agricultural sector. J. Reg. Sci. 60 (4), 612–627. https://doi.org/10.1111/jors.12474.
Karan, S.K., Woolf, D., Azzi, E.S. [Elias Sebastian], Sundberg, C., Wood, S.A., 2023. Potential for biochar carbon sequestration from crop residues: a global spatially explicit assessment. GCB Bioenergy 15 (12), 1424–1436. https://doi.org/10.1111/gcbb.13102.
Karananidi, P., Som, A.M., Loh, S.K., Bachmann, R.T., 2020. Flame curtain pyrolysis of oil palm fronds for potential acidic soil amelioration and climate change mitigation. J. Environ. Chem. Eng. 8 (4), 103982. https://doi.org/10.1016/j.jece.2020.103982.
Kirchem, D., Schill, W.-P., 2023. Power sector effects of green hydrogen production in Germany. Energy Policy 182, 113738. https://doi.org/10.1016/j.enpol.2023.113738.
Klaassen, R.E., Patel, M.K., 2013. District heating in the Netherlands today: A techno-economic assessment for NGCC-CHP (Natural Gas Combined Cycle combined heat and power). Energy 54, 63–73. https://doi.org/10.1016/j.energy.2013.02.034.
Lee, S., Moon, J., 2024. Feasibility Analysis of Applying Deep Neural Network on Driving Distance Estimation. IEEE Access 12, 81075–81087. https://doi.org/10.1109/ACCESS.2024.3410316.
Lefebvre, D., Fawzy, S., Aquije, C.A., Osman, A.I., Draper, K.T., Trabold, T.A., 2023. Biomass residue to carbon dioxide removal: quantifying the global impact of biochar. Biochar 5 (1). https://doi.org/10.1007/s42773-023-00258-2.
Lehmann, J., Cowie, A., Masiello, C.A., Kammann, C., Woolf, D., Amonette, J.E., Cayuela, M.L., Camps-Arbestain, M., Whitman, T., 2021. Biochar in climate change mitigation. Nat. Geosci. 14 (12), 883–892. https://doi.org/10.1038/s41561-021-00852-8.
Leppäkoski, L., Marttila, M.P., Uusitalo, V., Levänen, J., Halonen, V., Mikkilä, M.H., 2021. Assessing the carbon footprint of biochar from willow grown on marginal lands in Finland. Sustainability 13 (18), 10097. https://doi.org/10.3390/su131810097.
Letoffet, A., Campion, N., Böhme, M., Jensen, C.D., Ahrenfeldt, J., & Clausen, L.R. (2024). Techno-economic assessment of upgraded pyrolysis bio-oils for future marine fuels.
Li, W., Ciais, P., Makowski, D., & Peng, S. (2018). A global yield dataset for major lignocellulosic bioenergy crops based on field measurements. ⟨https://www.nature.com/articles/sdata2018169#Sec5⟩.

Li, Y. [Yuanchao], Zeng, H., Zhang, M., Wu, B., Zhao, Y., Yao, X., Cheng, T., Qin, X., Wu, F. [Fangming], 2023. A county-level soybean yield prediction framework coupled with XGBoost and multidimensional feature engineering. Int. J. Appl. Earth Obs. Geoinf. 118, 103269. https://doi.org/10.1016/j.jag.2023.103269.
Ma, Y., Woolf, D., Fan, M., Qiao, L., Li, R., Lehmann, J., 2023. Global crop production increase by soil organic carbon. Nat. Geosci. 16 (12), 1159–1165. https://doi.org/10.1038/s41561-023-01302-3.
Mehmooda, M.A., Ibrahim, M., Rashid, U., Nawaz, M., Ali, S., Hussain, A., & Gull, M. (2017). Biomass production for bioenergy using marginal lands.
Namaswa, T., Burslem, D.F., Smith, J., 2023. Emerging trends in appropriate kiln designs for small-scale biochar production in low to middle income countries. Bioresour. Technol. Rep. 24, 101641. https://doi.org/10.1016/j.biteb.2023.101641.
Noorunnahar, M., Chowdhury, A.H., Mila, F.A., 2023. A tree based eXtreme Gradient Boosting (XGBoost) machine learning model to forecast the annual rice production in Bangladesh. PloS One 18 (3), e0283452. https://doi.org/10.1371/journal.pone.0283452.
Nunes, L.J.R., Silva, S., 2023. Optimization of the residual biomass supply chain: process characterization and cost analysis. Logistics 7 (3), 48. https://doi.org/10.3390/logistics7030048.
Owsianiak, M., Lindhjem, H., CORNELISSEN, G., Hale, S.E. [Sarah E.], Sørmo, E., Sparrevik, M., 2021. Environmental and economic impacts of biochar production and agricultural use in six developing and middle-income countries. Sci. Total Environ. 755 (Pt 2), 142455. https://doi.org/10.1016/j.scitotenv.2020.142455.
Pandit, N.R., Mulder, J., Hale, S.E. [Sarah Elisabeth], Schmidt, H.P., Cornelissen, G., 2017. Biochar from "Kon Tiki" flame curtain and other kilns: Effects of nutrient enrichment and kiln type on crop yield and soil chemistry. PloS One 12 (4), e0176378. https://doi.org/10.1371/journal.pone.0176378.
Panoutsou, C., Chiaramonti, D., 2020. Socio-economic opportunities from miscanthus cultivation in marginal land for bioenergy. Energies 13 (11), 2741. https://doi.org/10.3390/en13112741.
Pedregosa, F., Varoquaux, G., Gramfort, A., Michel, V., Thirion, B., Grisel, O., Blonde, M., Prettenhofer, P., Weiss, R., Dubourg, V., Vanderplas, J., Passos, A., Cournapeau, D., Brucher, M., & Perrot, M. (2011). Scikit-learn: Machine Learning in Python.
Powis, C.M., Smith, S.M., Minx, J.C., Gasser, T., 2023. Quantifying global carbon dioxide removal deployment. Environ. Res. Lett. 18 (2), 24022. https://doi.org/10.1088/1748-9326/acb450.
PYREG. (2024, July 9). *Premium carbonization technology for a valuable business proposition.* ⟨https://pyreg.com/our-technology/⟩.
Romanelli, T.L., Cohen, M.J., Milan, M., & Brown, M.T. (2008). Emergy Synthesis of Intensice Eucalyptus Cultivation in Sao Paolo, Brazil.
Ruett, J., Abdelshafy, A., & Walther, G. (2024). Using miscanthus and biochar as sustainable substrates in horticulture: An economic and carbon footprint assessment of their primary and cascading value chains.
S2BIOM. (2012). *Tools for biomass chains - Data downloads.* ⟨https://s2biom.wenr.wur.nl/data-downloads⟩.
Sahoo, K., Bilek, E., Bergman, R., Mani, S., 2019. Techno-economic analysis of producing solid biofuels and biochar from forest residues using portable systems. Appl. Energy 235, 578–590. https://doi.org/10.1016/j.apenergy.2018.10.076.
Salo, H., Virtanen, S., Laine-Kaulio, H., Koivusalo, H., Jacques, D., Kokkonen, T., 2023. Evolution of pH, redox potential and solute concentrations in soil and drainage water at a cultivated acid sulfate soil profile. Geoderma 436, 116559. https://doi.org/10.1016/j.geoderma.2023.116559.
Schillerberg, T., Di Tian, 2023. Changes in crop failures and their predictions with agroclimatic conditions: analysis based on earth observations and machine learning over global croplands. Agric. For. Meteorol. 340, 109620. https://doi.org/10.1016/j.agrformet.2023.109620.
Smebye, A.B., Sparrevik, M., Schmidt, H.-P., & Cornelissen, G. (2017). Life-cycle assessment of biochar production systems in tropical rural areas: Comparing flame curtain kilns to other production methods.
Smith, S., Geden, O., Gidden, M., Lamb, W., Nemet, G., Minx, J., Buck, H., Burke, J., Cox, E., Edwards, M., Fuss, S., Johnstone, I., Müller-Hansen, F., Pongartz, J., Probst, B., Roe, S., Schenuit, F., Schulte, I., & Vaughan, N. (2024). The State of Carbon Dioxide Removal - 2nd Edition. *Chapter 5: Policy and Governance, the State of Carbon Dioxide Removal - 2nd Edition.* Advance online publication. https://doi.org/10.17605/OSF.IO/F85QJ.
Song, S., Liu, Z. [Zhaoxia], Liu, G., Cui, X., Sun, J., 2023. Application of biochar cement-based materials for carbon sequestration. Constr. Build. Mater. 405, 133373. https://doi.org/10.1016/j.conbuildmat.2023.133373.
Sørmo, E., Silvani, L., Thune, G., Gerber, H., Schmidt, H.P., Smebye, A.B., CORNELISSEN, G., 2020. Waste timber pyrolysis in a medium-scale unit: Emission budgets and biochar quality. Sci. Total Environ. 718, 137335. https://doi.org/10.1016/j.scitotenv.2020.137335.
Sousa, L.M. de, Poggio, L., Batjes, N.H., Heuvelink, G.B.M., Kempen, B., Riberio, E., & Rossiter, D. (2020). *SoilGrids 2.0: producing quality-assessed soil information for the globe.* https://doi.org/10.5194/soil-2020-65.
Tang, Y., Li, Y. [Yue], Cockerill, T.T., 2024. Environmental and economic spatial analysis system for biochar production – case studies in the East of England and the East Midlands. Biomass.. Bioenergy 184, 107187. https://doi.org/10.1016/j.biombioe.2024.107187.
Torres-Morales, E., Khatiwada, D., Xylia, M., Johnson, F.X., 2023. Investigating biochar as a net-negative emissions strategy in Colombia: Potentials, costs, and barriers. Curr. Res. Environ. Sustain. 6, 100229. https://doi.org/10.1016/j.crsust.2023.100229.
Tribe, M.A., & Alpine, R. (1986). Scale economies and the "0.6 rule".
Wagner, M., Winkler, B., Lask, J., Weik, J., Kiesel, A., Koch, M., Clifton-Brown, J., Cossel, M. von, 2022. The true costs and benefits of miscanthus cultivation. Agronomy 12 (12), 3071. https://doi.org/10.3390/agronomy12123071.
Wallikhani, A.H., Asakereh, A., Farrokhian Firouzi, A., 2022. Biochar and bioenergy production by pyrolysis of Conocarpus and Eucalyptus wastes: a case study, Khuzestan province, Iran. Int. J. Environ. Sci. Technol. 19 (7), 5839–5848. https://doi.org/10.1007/s13762-021-03765-6.
Wang, Y. [Yang], Lin, Q., Liu, Z. [Zhongzhen], Liu, K., Wang, X., Shang, J., 2023. Salt-affected marginal lands: a solution for biochar production. Biochar 5 (1). https://doi.org/10.1007/s42773-023-00219-9.
Winkler, B., Mangold, A., Cossel, M. von, Clifton-Brown, J., Pogrzeba, M., Lewandowski, I., Iqbal, Y., Kiesel, A., 2020. Implementing miscanthus into farming systems: A review of agronomic practices, capital and labour demand. Renew. Sustain. Energy Rev. 132, 110053. https://doi.org/10.1016/j.rser.2020.110053.
Wolniak, R., Skotnicka-Zasadzień, B., 2023. Development of Wind Energy in EU Countries as an Alternative Resource to Fossil Fuels in the Years 2016–2022. Resources 12 (8), 96. https://doi.org/10.3390/resources12080096.
World Bank Group. (2024, October 31). *GDP per capita (current US$).* ⟨https://data.worldbank.org/indicator/NY.GDP.PCAP.CD⟩.
Worldclim. (2020). *Historical climate data.* ⟨https://www.worldclim.org/data/worldclim21.html⟩.
Xu, D., Wang, Y. [Yinuo], Hu, H., Yellezuome, D., He, F., & Cai, J. (2024). Energy consumption balance and environmental benefits from the pyrolysis of switchgrass cultivated on marginal lands with biochar application to soil in China.
Yakubu, S., Jaiyeoba, I.A., Gasu, M.B., Yakubu, D.A., 2021. Variability of soil properties under continuous irrigation farming in Nigerian Savanna. J. Cameroon Acad. Sci. 17 (1), 59–68. https://doi.org/10.4314/jcas.v17i1.4.
Zhao, X., Kang, L., Wang, Q., Lin, C., Liu, W., Chen, W., Sang, T., Yan, J., 2021. Water use efficiency and stress tolerance of the potential energy crop miscanthus lutarioriparius grown on the Loess Plateau of China. Plants (Basel Switz.) 10 (3). https://doi.org/10.3390/plants10030544.
Zhou, N., Zhou, J., Dai, L., Guo, F., Wang, Y. [Yunpu], Li, H., Deng, W., Lei, H., Chen, P., Liu, Y., Ruan, R., 2020. Syngas production from biomass pyrolysis in a continuous microwave assisted pyrolysis system. Bioresour. Technol. 314, 123756. https://doi.org/10.1016/j.biortech.2020.123756.